*American Mineralogist, Volume 92, pages 1665–1672, 2007*

# Acoustic dissipation associated with phase transitions in lawsonite, $CaAl_2Si_2O_7(OH)_2 \cdot H_2O$

**Ruth E.A. McKnight,[1,*] Michael A. Carpenter,[1] Tim W. Darling,[2] Andy Buckley,[1] and Paul A. Taylor[1]**

[1]Department of Earth Sciences, University of Cambridge, Downing Street, Cambridge, CB2 3EQ, U.K.
[2]Department of Physics, University of Nevada, Reno, Nevada 89577, U.S.A.

## Abstract

Resonant ultrasound spectra of a single crystal and a polycrystalline sample of lawsonite [$CaAl_2Si_2O_7(OH)_2 \cdot H_2O$] have been measured at room temperature and at low temperatures in the region 20–300 K. The influence of known phase transitions at 125 and 270 K is seen in the frequency variations of the resonance peaks, which are indicative of elastic stiffening, and in values for the quality factor $Q_{QF}$, which are indicative of dissipation. Two dissipation peaks, at ~250 and ~210 K, are interpreted as being due to the proton order-disorder processes associated with the two species of hydrogen atoms in the structure: one in hydroxyl OH groups and one in the $H_2O$ molecules. These occur below the *Cmcm* ↔ *Pmcn* transition point but coincide with changes in the shear elastic constants and in features of IR spectra reported elsewhere. A third, much smaller, dissipation peak occurs immediately below the *Pmcn* ↔ $P2_1cn$ transition point. The combination of these anomalies in acoustic dissipation and in elastic constants is consistent with the view that the *Cmcm* ↔ *Pmcn* transition is driven both by displacive and proton ordering effects. For the *Pmcn* ↔ $P2_1cn$ transition, dissipation and the transition are more closely related, consistent with the view that the transition is driven essentially by proton ordering.

**Keywords:** Lawsonite, resonant ultrasound spectroscopy, dissipation, proton ordering

## Introduction

Lawsonite [$CaAl_2Si_2O_7(OH)_2 \cdot H_2O$] is of interest in Earth sciences due to its unusually high water content (~11.5 wt% $H_2O$) and high density. It is formed from hydration of the anorthite component of rocks in regions of high-pressure, low-temperature metamorphism, and has a wide *P-T* stability field (Schmidt 1995). It is therefore considered to be a significant mineral for possible transport of water into the mantle at subduction zones (Chatterjee and Leistner 1984; Pawley 1994; Pawley et al. 1996; Schmidt and Poli 1998; Schilling et al. 2003). It also has a high degree of shear anisotropy, resulting in a distinctive seismic signature when it is present in abundance at depth in the Earth (Sinogeikin et al. 2000).

Lawsonite undergoes two reversible phase transitions at low temperature associated with rearrangement of hydrogen bonds within the structure (Libowitzky and Armbruster 1995; Libowitzky and Rossman 1996). At 270 K, there is a transition from the room temperature orthorhombic *Cmcm* structure, with dynamically disordered hydroxyl OH groups and $H_2O$ molecules, to the *Pmcn* phase in which $H_2O$ and OH groups are systematically rotated within the (100) plane, thus strengthening some hydrogen bonds and weakening others. The *Pmcn* structure persists to 125 K in a natural sample (155 K in a deuterated sample), where there is a transition to a polar (ferroelectric) $P2_1cn$ structure due to unidirectional shifts of the hydrogen atoms of the $H_2O$ and OH groups along the **x** axis (Libowitzky and Armbruster 1995; Carpenter et al. 2003). The 270 K transition is tricritical in character and the 125 K transition is second order, but the thermodynamic properties do not follow exactly the expected behavior for classical tricritical and second-order transitions (Sondergeld et al. 2000a, 2000b, 2005; Meyer et al. 2000, 2001; Martín-Ollala et al. 2001; Hayward et al. 2002; Carpenter et al. 2003; Schranz et al. 2005).

The symmetry changes at the two phase transitions have been investigated in great detail using X-ray diffraction (Libowitzky and Armbruster 1995) and FTIR spectroscopy (Libowitzky and Rossman 1996). Further works on lawsonite using X-ray diffraction (Sondergeld et al. 2005; Schranz et al. 2005), strain analysis (Carpenter et al. 2003), calorimetry (Martín-Olalla et al. 2001; Hayward et al. 2002), transmission electron microscopy (Cámara et al. 2001), and optical, elastic, and dielectric studies (Sondergeld et al. 2000b, 2005) have confirmed the occurrence of these phase transitions and the anomalies observed due to changes in the hydrogen bonds within the structure. Powder neutron diffraction studies (Meyer et al. 2001; Carpenter et al. 2003) and infrared spectroscopy experiments (Meyer et al. 2000) have shown that displacive components involving framework distortions and proton ordering may contribute differently to the two phase transitions.

The temperature dependencies of the elastic constants of single crystals of lawsonite have been examined using Brillouin spectroscopy and plane wave resonance (Sinogeikin et al. 2000; Schilling et al. 2003; Sondergeld et al. 2005; Carpenter 2006). As a result of the phase transitions, the elastic constants show a complex pattern of softening and stiffening that depends on the

* E-mail: ream3@cam.ac.uk

coupling of the strain with both cation ordering and displacive processes. The variations in elastic properties are of specific interest, as they can provide insights into the mechanisms of the phase transitions and hence into the interaction of hydrogen atoms with an aluminosilicate framework.

In this study, resonant ultrasound spectroscopy (RUS) (Migliori et al. 1993, 2001; Maynard 1996; Leisure and Willis 1997; Migliori and Maynard 2005) was used to examine temperature-dependent anomalies in acoustic dissipation for single-crystal and polycrystalline lawsonite samples. The main objective was to investigate the possibility that dissipation processes associated with proton dynamics could be observed by RUS. Lawsonite was chosen for this purpose because of its large changes in hydrogen bonding and topology of water molecules, which are already known from previous studies. The fundamental principle being tested is that changes in proton (or deuterium) configurations give rise to changes in lattice parameters and hence that, conversely, externally applied stresses should modify the proton configurations. If the applied stress is dynamical, as in an acoustic resonance experiment, there should be frequency and temperature ranges over which strong anelastic effects might arise due to proton movements between related crystallographic sites. These are expected to result in peaks in the variations of mechanical quality factor, $Q_{QF}$ (the subscripts are added throughout this paper to distinguish between quality factor, $Q_{QF}$, and the order parameter $Q_{OP}$), as extracted from line widths of the resonance spectra.

## Experimental details

### Apparatus

A low-temperature RUS setup was used for this experiment. It consists of a standard RUS arrangement controlled by a Dynamic Resonance System (DRS) Modulus II system. A sample of lawsonite in the shape of a parallelepiped is mounted on its opposite corners between two piezoelectric transducers, one of which acts as the resonator and the other as the detector. The RUS head itself is a new design, as shown in Figure 1, and is made mainly from Tufnol composite G10/40 to reduce mechanical linkages between the transducers other than through the sample, even at low temperatures. The bottom piezoelectric transducer is shielded with copper foil to reduce radio frequency interference. The whole RUS head is mounted on the end of a stick and lowered into a standard Orange 50 mm helium flow cryostat, supplied by AS Scientific Products Ltd. Temperature regulation and measurement is achieved using a silicon diode and a LakeShore model 340 controller. All materials for elements used in the system, including the wires connecting the RUS head to the computer, were specially selected so that they operated well down to temperatures as low as ~5 K. Data can be collected during cooling and heating cycles in a temperature range of ~5–300 K with the temperature stability for each measurement being approximately ±0.1 K.

### Sample description

The polycrystalline lawsonite sample used in this study was taken from a vein several centimeters wide in a blueschist rock from Valley Ford, Sonoma County, California and is number 120943 of the Harvard University mineral collection, provided by C. Francis (Harvard University, U.S.A.). It contains ~98% lawsonite and ~2% calcite. The composition of the lawsonite, from probe analysis, is $Ca_{1.00}Al_{1.95}Fe_{0.05}Si_{2.00}O_7(OH)_2 \cdot H_2O$. This sample has been described in detail by Martín-Olalla et al. (2001). Examination of a thin section shows that the sample has grain sizes in the range ~0.1 to ~5 mm. Slices from the same hand specimen were examined in the TEM by Cámara et al. (2001), where it was found to have a large concentration of dislocations throughout. However, characterization of dislocation behavior across the phase transitions was not possible in the study due to the high mobility of protons under the electron beam.

The single-crystal lawsonite sample used is number 108762 from the Harvard University mineral collection, also provided by C. Francis. It is from the type locality near Reed Station, Tiburon Peninsula, Marin County, California. The crystal used was white in color with a small proportion of fine inclusions, mostly of a brownish red color. The parallelepiped was cut in such a way as to try and minimize the number of impurities.

Parallelepipeds with orthogonal faces were cut from both lawsonite samples using an annular diamond saw, lubricated with paraffin. For this purpose, the samples were glued to glass blocks using Crystalbond glue, manufactured by SPI supplies, with a working point of 120–130 °C. Several parallelepipeds were cut from the polycrystalline sample. These appeared to contain some fine cracks. The parallelepiped chosen for low temperature measurements had dimensions 4.753 × 4.318 × 3.753 mm and a weight of 0.2304 g. Two faces of the single-crystal parallelepiped were cut parallel to the (010) crystallographic plane and the other two edges were arbitrary orientations perpendicular to (010). The dimensions were 1.483 × 2.148 × 2.342 mm and the sample weighed 0.0229 g.

### Data collection

For the purposes of this study, separate RUS measurements were made at room temperature and at low temperatures, as follows.

**Room temperature.** The RUS spectra of several polycrystalline parallelepipeds and one single-crystal sample were individually measured using a commercial DRS head. Each sample was measured in four different orientations to ensure that all resonances in the spectra were excited and observed. Spectra from the polycrystalline sample were measured in the frequency range 0.1–1.2 MHz, with 20 000 data points. The single crystal was measured in the range 0.05–2 MHz with 50 000 data points. The room-temperature spectra for the polycrystalline lawsonite samples gave some indication of which parallelepiped was likely to give the most information during low temperature measurements. Selection of the particular sample used for low-temperature measurements was based on the spectra for that

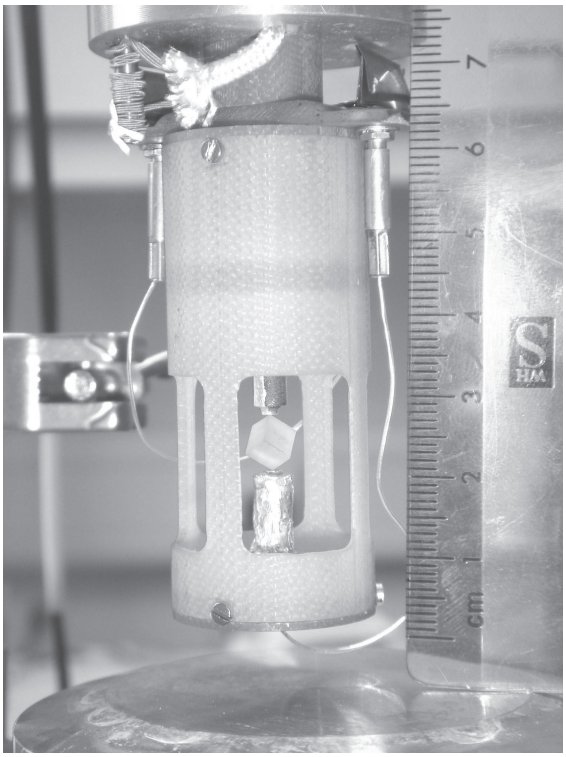


**Figure 1.** The new design of the RUS head for low-temperature studies. It is a regular RUS setup where the sample is mounted between two piezoelectric transducers; however, the head is mounted in Tufnol G10/40 composite to minimize mechanical linkages, and the bottom transducer has been shielded with copper foil to reduce radio interference. The head is attached to a long stick to be lowered into the cryostat. A scale bar is shown for reference.

parallelepiped having the sharpest peaks and optical examination showing the least number of cracks. The frequency ranges for measurements depend on sample size and were chosen based on preliminary checks to see where the resonance peaks occurred for each sample.

**Low temperature.** For measurements at low temperature, the sample was mounted on the low-temperature head, as shown in Figure 1. The head was lowered into the cryostat, which was then sealed and vacuum pumped. The cryogens were added after the sample had been inserted and the sample chamber was filled with ~1.3 mbar of He gas to allow heat exchange between the sample and cryostat. For the polycrystalline sample, the system was cooled in 20 K intervals from 290 to 50 K with a 15 min pause at each step to equilibrate both the sample and the RUS head at progressively lower temperatures without imposing large thermal shocks. After the equilibration time at each step, a RUS spectrum was measured in the frequency range 0.1–1.5 MHz with 65 000 data points. For the single crystal, the system was cooled in 20 K stages from 120 to 20 K with a 15 min settle time at each temperature. Spectra were measured at each step in the frequency range 0.3–2 MHz with 65 000 data points.

The samples were then heated up again to 300 K in 5 K steps, each with a settle time of 15 min, and a spectrum was measured at each step. The 15 min settle time for each temperature was chosen based on previous observations of how long it took for the sample to equilibrate at each temperature step. Spectra were taken in the same frequency ranges and with the same number of data points as during the cooling cycle.

All spectra measured using the DRS software were transferred to the software program Igor for data analysis. A plot of all spectra (amplitude as a function of frequency) stacked as a function of temperature in small temperature intervals provides an easy way to observe and follow the trends of resonant frequencies as they evolve with temperature. Quantitative calculations of peak positions and peak halfwidths were then carried out by fitting an asymmetric Lorentzian function to each peak (Schreuer et al. 2003; Schreuer and Thybaut 2005). The mechanical quality factor, $Q_{QF}$, is given by $Q_{QF} = f/\Delta f$, where $f$ is the peak frequency, and $\Delta f$ is the peak width at the half-maximum point.

## Experimental results

### Room-temperature experiments

Room-temperature spectra for polycrystalline and single-crystal lawsonite (Figs. 2a and 2b, respectively) both show weak, broad peaks. The mechanical quality factor $Q_{QF}$ is below 100 for all resonances in the polycrystalline spectra, and is still low for the single crystal at around 300.

It was not possible to make accurate measurements of the positions for all peaks in spectra from the polycrystalline sample, but attempts were made to fit a selection of the more well-defined ones with bulk and shear moduli, using the DRS software and assuming an isotropic medium. Starting values for the fit were the Hill averages for bulk and shear moduli calculated by Sinogeikin et al. (2000). However, these failed to give an internally consistent fit to the peak frequencies, due either to the presence of cracks or to the fact that the sample did not contain a sufficient number of separate, randomly oriented grains to be isotropic. Peaks in spectra from the single crystal are better resolved, but the data were of not sufficient quality to allow fitting of elastic constants.

### Low-temperature experiments

**Polycrystalline lawsonite.** Figure 3 shows a stack of spectra for the polycrystalline lawsonite sample as it was heated from 50 to 300 K in 5 K intervals. The broad room-temperature peaks sharpen toward lower temperatures. The frequencies of these peaks clearly vary substantially (by up to 140 kHz in some cases) between 50 K and room temperature, and the variation is not a linear function of temperature but shows marked curvature. The trends of selected peaks, picked out by inspection, are shown by

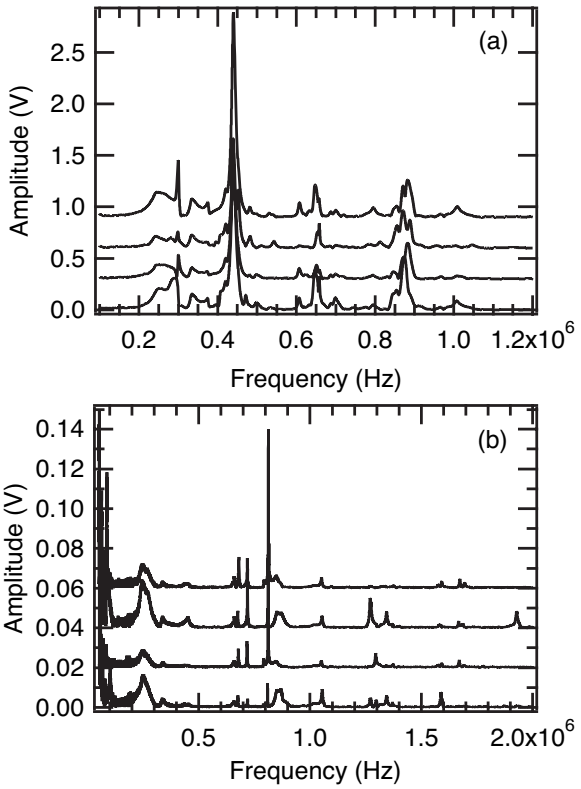


**Figure 2.** Room-temperature spectra for (**a**) the polycrystalline parallelepiped and (**b**) the single-crystal sample. The four separate spectra in each figure represent the lawsonite samples oriented in four different directions so that as many resonances as possible are excited.

hatched gray curves added to Figure 3. The two known transitions at 125 and 270 K are indicated by dark lines. On heating from 50 K, the peaks vary toward lower frequencies slightly and cross the 125 K transition with no obvious deviation from this trend. The trend then changes direction about 30 K above the transition point (~155 K) and there is a maximum in all the peak frequencies at approximately 210 K. There is significant peak broadening at this point, although there is a general trend of peak broadening on heating across the whole temperature range. The frequencies then decrease toward the 270 K phase transition but there is another change in direction where they start to increase again at about 255 K. There is a steady increase in peak frequencies from ~255 K across the 270 K transition and a slight flattening toward room temperature.

Figure 4a shows the peak positions that were measured for peaks 1–7 in Figure 3. The slight change in slope just above the 125 K transition, the minimum ~20 K below the 270 K transition and the maximum at ~225 K are clearly visible in the evolution of all the peaks. The variations of $Q_{QF}$, and its inverse $Q_{QF}^{-1}$ for these peaks are shown in Figures 4b and 4c. The known phase transitions at 270 and 125 K are marked with dashed lines. The variation in $Q_{QF}$ shows a more or less linear decrease on heating from 50 K to approximately 130 K where there is a definite change in the slope. This corresponds to the known $Pmcn \leftrightarrow P2_1cn$ phase transition. There is then a second break in slope at ~225 K, which appears to correspond with a peak in the varia-

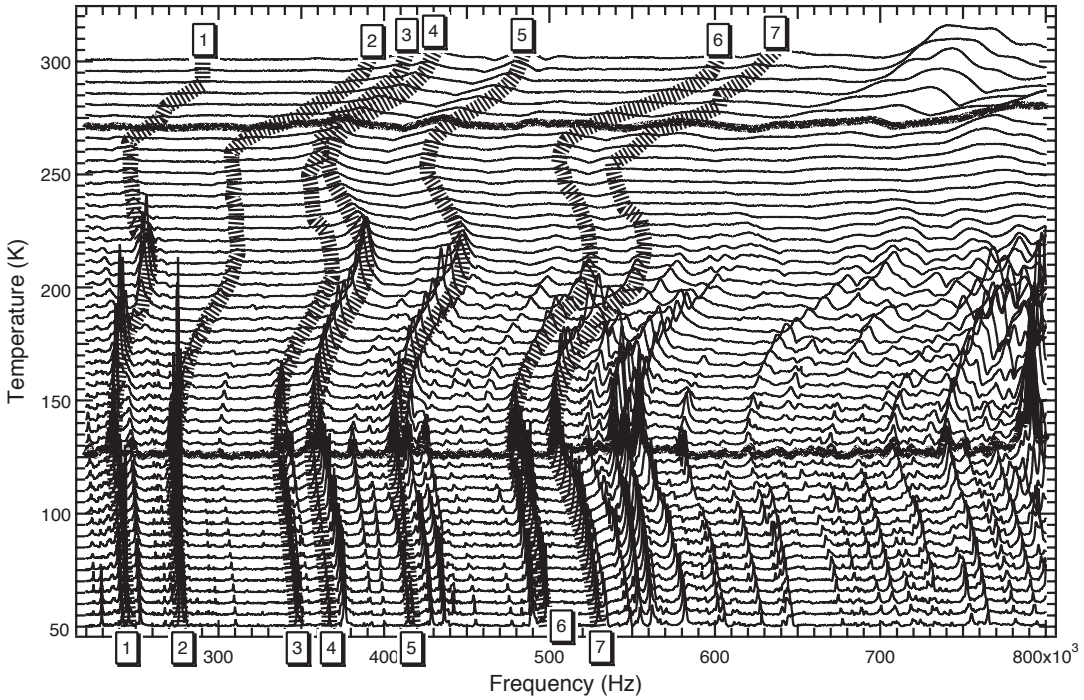


**FIGURE 3.** RUS spectra for polycrystalline lawsonite at 5 K intervals on heating through the temperature range 50–300 K. Spectra in bold at 270 and 125 K mark the two phase transitions that are known to occur in lawsonite. Gray hatched lines have been added as guides to the eye for the evolution of individual peaks. Some resonance peaks that have been followed through the whole temperature range have been numbered.

tions of frequency shown in Figure 4a. $Q_{QF}$ then stays very low and approximately constant up to room temperature. The scatter in $Q_{QF}$ values is an indication of experimental uncertainty at each temperature.

It is more common to use the inverse of the quality factor, $Q_{QF}^{-1}$, as this is directly related to dissipation in the sample. Figure 4c shows $Q_{QF}^{-1}$ plotted as a function of temperature. There is no obvious deviation in $Q_{QF}^{-1}$ at the 125 K transition point; however there is a clear break in slope at approximately 225 K. From the general trend of $Q_{QF}^{-1}$, it appears that there is a maximum at or just below the 270 K transition temperature.

**Single-crystal lawsonite.** Figure 5 shows a stack of RUS spectra taken during heating of the single-crystal lawsonite sample from 20 to 300 K in 5 K intervals. The spectra at 125 and 270 K, where the phase transitions are known to occur, are marked in bold. Hatched gray lines trace the evolution of the resonance peaks with temperature, and are clearly non-linear functions of temperature. The peaks show a marked curvature toward lower frequencies as the sample is heated toward both of the transitions, indicating elastic softening. For example, peak 7 decreases in frequency by approximately 0.2 MHz between 20 K and the 125 K transition point. At 125 K, the trends level out and the peaks decrease in frequency only slightly as temperature increases. At about 230 K, there is another marked reduction in frequency (elastic softening) as the sample approaches the second transition at 270 K. This time, the frequency of peak 7 decreases by ~0.1 MHz. When the transition point is reached, the peak evolution changes direction and there is a small but noticeable trend toward higher frequencies up to 300 K. All resonance peaks appear to follow this trend. There are also changes in line widths as a function of temperature. The peaks remain relatively sharp from 20 K up to the first transition at 125 K, but there is significant broadening toward the 270 K transition, at which point the peaks seem to sharpen up again on approaching room temperature.

The frequencies of peaks 1–10 from Figure 5 and values of $Q_{QF}$ for peaks 1, 2, 4, and 10, obtained from peak fitting, are shown in Figure 6. The two known phase transitions are indicated by gray dashed lines. Figure 6a shows that the evolution toward lower frequencies in the region below each of the two phase transitions is followed by all the resonance peaks. They then level off and increase or remain more or less constant above ~270 K.

Values of $Q_{QF}$ clearly decrease on heating across the temperature range (Fig. 6b); however, the 125 K transition appears to be marked by a peak. There is a minimum in $Q_{QF}$ at approximately 210 K followed by a small maximum at ~220 K. There is another minimum about 20 K below the 270 K transition point, followed by an increase in $Q_{QF}$, which seems to plateau at the 270 K phase transition. Figure 6c provides an alternative perspective showing the evolution of $Q_{QF}^{-1}$. The level of dissipation appears to be approximately constant at low temperatures, until there is a small peak just below the first phase transition at ~120 K (expanded for clarity as an insert in Fig. 6c). The dissipation then increases above 125 K with clear maxima at ~210 and ~250 K, before declining steadily above ~250 K.

## DISCUSSION

There are several things to take account of from the results presented here. First, the frequency variations are of interest as

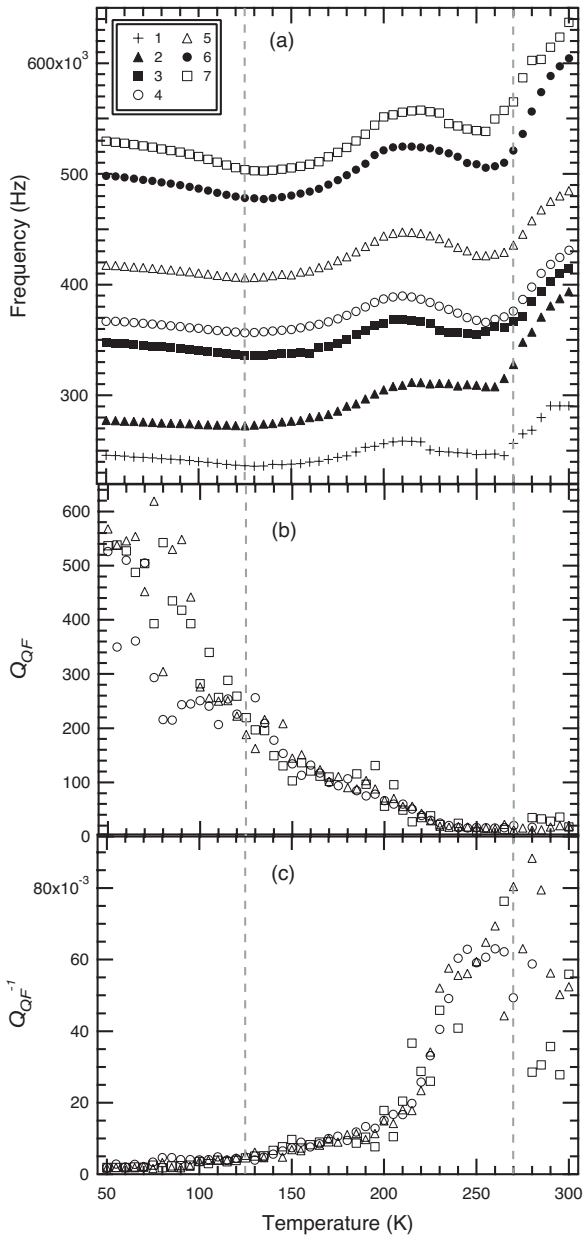


**FIGURE 4.** Variations of (**a**) peak frequencies, (**b**) quality factor $Q_{QF}$, and (**c**) inverse quality $Q_{QF}^{-1}$, as extracted from the primary spectra shown in Figure 3 for the polycrystalline sample. Numbers correspond to the labels in Figure 3.

they are directly related to variations of elastic constants. Second, the trends in $Q_{QF}$ and $Q_{QF}^{-1}$ provide information on the dissipation processes in the sample. Finally, these can be compared with results from other experiments on lawsonite to provide new information on the atomic scale processes involved in the phase transitions.

### Elastic constant variations

Increases in resonant frequencies with falling temperature imply stiffening of the elastic constants in a non-linear manner that is closely similar to the pattern of single-crystal elastic constants measured by Sondergeld et al. (2005). In general for RUS, individual resonances are controlled predominantly by different combinations of shear elastic constants and are influenced to a much lesser extent by compressional distortions. It can be noted, for example, that the softening with falling temperature above 270 K that is seen in almost all resonances in both polycrystalline and single-crystal lawsonite spectra can only be seen in the $C_{66}$ mode for single-crystal data given by Schilling et al. (2003) and Sondergeld et al. (2005). Peak 9 clearly has a large component of $C_{66}$ as it stiffens significantly, whereas peak 4 is less influenced by $C_{66}$. For an isotropic material the resonances are expected to behave more uniformly as each is determined by the shear modulus, which is an effective average of the single-crystal elastic constants.

Migliori and Sarrao (1997) note that the square of a resonant frequency gives the effective elastic modulus $C_{eff}$ associated with that mode. The lowest frequency modes tend to be virtually pure shear, so that their resonance frequencies can be used to provide indirect information about the evolution of the order parameter, $Q_{OP}$. For each of $C_{44}$, $C_{55}$, and $C_{66}$ the expected relationship is $\Delta C_{ii} \propto Q_{OP}^2$, where $\Delta C_{ii} = C_{ii} - C_{ii}^0$. $C_{ii}$ refers to the low symmetry phase and $C_{ii}^0$ refers to the high symmetry phase at each transition (Sondergeld al. 2005, Carpenter 2006). Straight lines were fit to the square of the frequencies ($\propto C_{eff}$) for each resonance peak above 270 K to determine the variation of $f_0^2$ (corresponding to some related set of elastic constants of the high symmetry phase). These were then extrapolated into the temperature range of the lower symmetry phases to give a measure of $\Delta f^2 = f^2 - f_0^2$, where $f^2$ is the square of the frequency of the peak in the low symmetry phase and $f_0^2$ is the extrapolated frequency squared at that temperature from the high symmetry phase. A similar calculation has been done to follow the evolution of the single-crystal elastic constants by Carpenter (2006). Figure 7 shows the deviation of the square of the excess squared frequency, $(\Delta f^2)^2$, away from the straight line fit to data above ~270 K. There is an approximately linear trend from 270 K down to the 125 K transition point for all resonances. This is consistent both with the assumption that frequency is an approximately linear function of the elastic constants and with the known tricritical character for the 270 K transition (i.e., $Q_{OP}^4 \propto T$). Significantly, however, the data in Figure 7 tend to zero about 10 K below the known transition temperature of 270 K, implying that the mechanism for elastic stiffening does not become established until ~10 K below $T_c$. In contrast, stiffening at the low temperature (125 K) transition develops directly at the transition point (Fig. 5).

### Mechanical quality factor, $Q_{QF}$, variations

Variations in $Q_{QF}$ are due to variations of acoustic dissipation or attenuation in the structure. A low $Q_{QF}$ value implies a large amount of dissipation and, inversely, high $Q_{QF}$ means the dissipation is low. The general trends in $Q_{QF}$ are similar in the single-crystal and polycrystalline samples. The single-crystal spectra have much better resolution (i.e., sharper, stronger peaks) than those for the polycrystalline sample and more information can therefore be gained from the former. Both have a large peak in the evolution of $Q_{QF}^{-1}$ at ~250 K, just below the 270 K phase transition. The peak is perhaps slightly frequency-dependent.

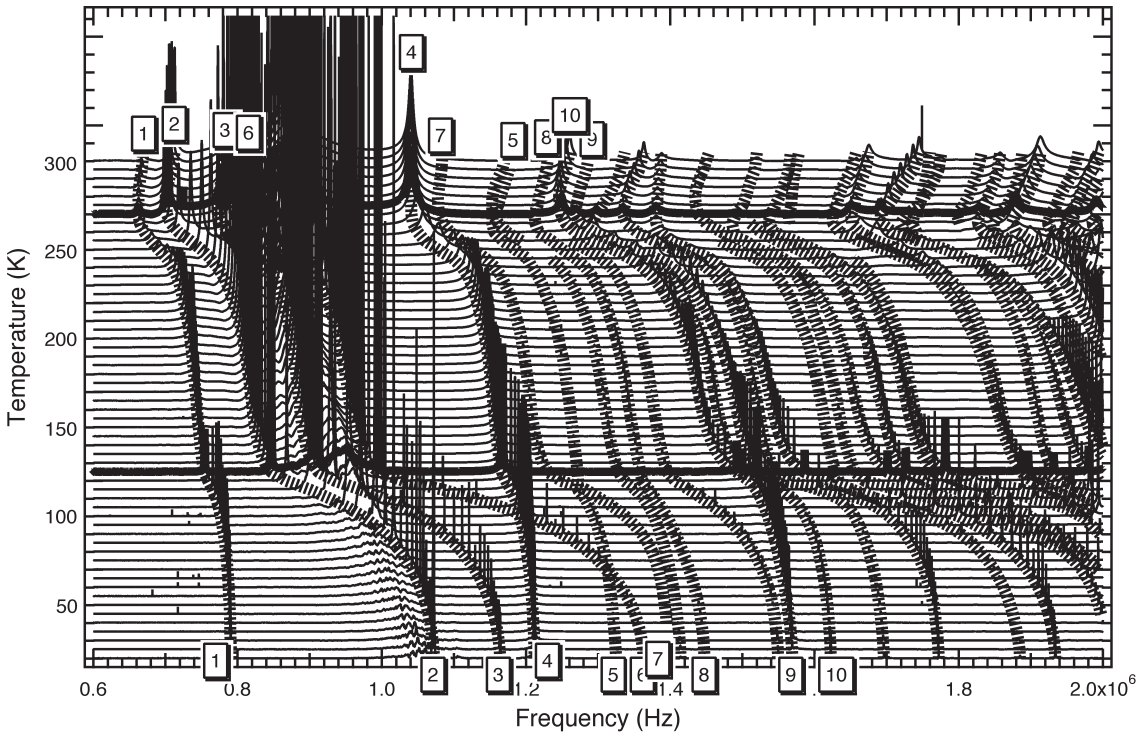


**FIGURE 5.** RUS spectra for single-crystal lawsonite at 5 K intervals on heating through the temperature range 20–300 K. Spectra in bold at 270 and 125 K mark the two phase transitions that are known to occur in lawsonite. Gray hatched lines have been added as guides to the eye for the evolution of individual peaks. Some resonance peaks that have been followed through the whole temperature range have been numbered.

These types of peaks, called "Snoek relaxation peaks" (Snoek 1941; Nowick and Berry 1972), have been observed in metals and ceramics (Leisure and Willis 1997; Leisure et al. 2004; Schreuer 2006). They are explained in terms of some temperature-dependent dynamical process that has a peak in the acoustic dissipation caused by an elastic relaxation when the frequency of the relaxation process becomes similar to that of the externally applied stress. For example, proton-hopping between preferred positions in a structure can be a temperature-activated process that will cause such a dissipation peak. At temperatures above the peak, the protons move freely between preferred positions because the timescale of the applied stress is slower than the proton-hopping rate. At temperatures below the peak, the protons are effectively frozen in place because the timescale of vibration is too fast for them to be able to respond to the external stress. Arrhenius plots based on the temperature at which there is a peak in $Q_{QF}^{-1}$, as determined for different frequencies yield an activation energy, and therefore help to understand what process is causing the dissipation peak. Figure 8 shows an Arrhenius plot for the peak at ~250 K in the single-crystal data. The frequency range is not sufficient to yield a reliable activation energy, but the data at least imply either that the dissipation mechanism is not thermally activated or that the activation energy is very low. As a guide to the eye, the straight line fit to the data gives an activation energy of 12 kJ/mol. In contrast with the original Snoek effect, where impurity atoms in a metal occupy interstitial positions, the protons in lawsonite are at crystallographic sites. At high temperatures they occupy single sites, on average, but these become split positions once symmetry is broken. The dynamical process envisaged here is hopping across a small energy barrier between the split positions.

Similar peaks are also visible in the single-crystal data at two other temperatures, ~210 and ~120 K, though neither of these show any variation in peak temperature as a function of frequency. As there are two different species of protons in the lawsonite structure (one in OH groups and one in $H_2O$ molecules) it is possible that the two peaks in the stability field of the *Pmcn* phase are associated with two different sets of energetics and dynamics of proton motions. The anomaly in $Q_{QF}^{-1}$ at ~120 K is much smaller and located immediately below $T_c$ (Fig. 6c insert). This tighter association with the transition point could mean that the dissipation is due to the normal dynamical processes, which occur in the vicinity of a displacive phase transition, rather than specifically to proton motions.

### Comparison with previous results

Previous studies on single crystals of lawsonite have shown the same pattern of stiffening once the temperature is reduced to ~20 K below the 270 K transition point rather than the abrupt softening which is normally expected for a tricritical displacive phase transition (Sondergeld et al. 2005; Carpenter 2006). It is easy to envisage that a pattern of ordered hydrogen bonds would act as braces for a framework structure and would therefore cause elastic stiffening. It has previously been proposed that the 270 K phase transition involves a combination of displacive and order-disorder processes (Meyer et al. 2000, 2001; Carpenter et al. 2003; Carpenter 2006) so it is possible that, although the displacement of atoms occurs at the phase transition, the actual

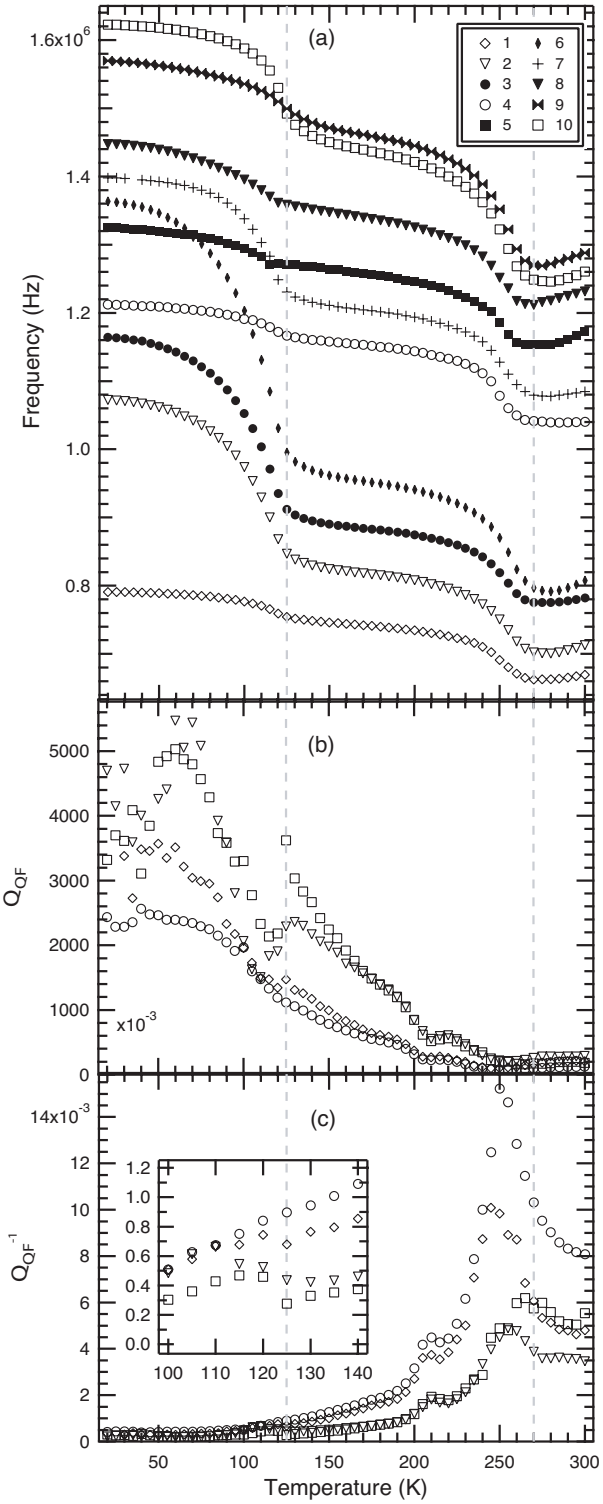


**FIGURE 6.** Variations of (**a**) peak frequencies, (**b**) quality factor $Q_{QF}$, and (**c**) inverse quality $Q_{QF}^{-1}$, as extracted from the primary spectra shown in Figure 5 for the single-crystal sample. Numbers correspond to the labels in Figure 5. The insert in **c** is an expanded section of the $Q_{QF}^{-1}$ variation in the temperature region 98–142 K, showing the small peak in $Q_{QF}^{-1}$ as a function of temperature in the region of the 125 K phase transition.

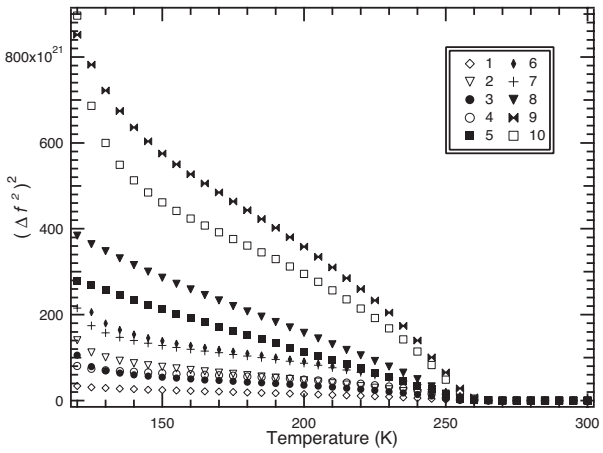


**FIGURE 7.** Temperature dependence of $(\Delta f^2)^2$ across the *Cmcm* ↔ *Pmcn* transition, where $(\Delta f^2)$ is the change in the squared resonance frequency of the *Pmcn* structure relative to that of the *Cmcm* structure extrapolated below ~270 K. Numbers correspond to those in Figure 6a. Note that $(\Delta f^2)^2$ extrapolates to zero approximately 10–20 K below 270 K.

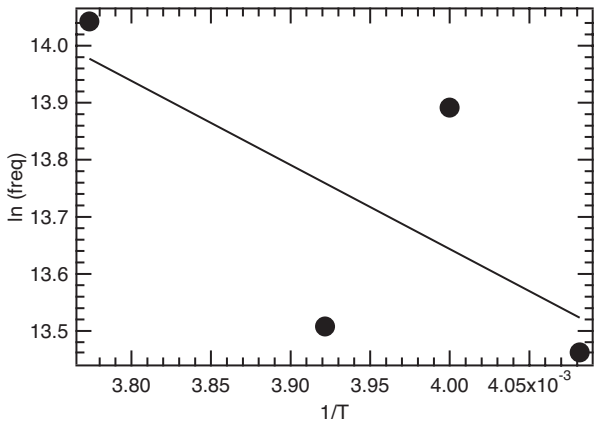


**FIGURE 8.** Arrhenius plot for the Snoek-like peaks in $Q_{QF}^{-1}$ for single-crystal lawsonite in the region just below the 270 K phase transition point at around 250 K. Data points refer to the peak temperatures of the peaks in $Q_{QF}^{-1}$ at four different frequencies. The activation obtained from the straight line fit is 12 kJ/mol, but this is clearly not well constrained.

proton ordering takes place at temperatures slightly below the transition point, causing a curvature in the elastic properties and a peak in the dissipation.

Anomalies in the region of ~200–225 K have previously been observed by other experimental methods, and these may be related to the dissipation peak that is observed here at ~210 K. The evolution of the frequency of the ~3600 $cm^{-1}$ absorption band in IR spectra below room temperature shows a kink just above ~200 K (Meyer et al. 2000). Single-crystal elastic constant data also show kinks in $C_{44}$ and $C_{55}$ near 208 K (Sondergeld et al. 2005). Strain analysis shows a small anomaly in the data for a natural sample at ~225 K, which increases to ~250 K when the sample is deuterated (Carpenter et al. 2003). This suggests that additional structural changes associated with proton ordering develop well within the stability field of the *Pmcn* structure. A break in slope at

this temperature is also seen in the variation of the square of the average intensity of superlattice reflections from single-crystal X-ray diffraction patterns (Sondergeld et al. 2005).

By way of contrast, the lower temperature transition is marked by a uniform pattern of elastic stiffening, changes in strain and changes in IR spectral parameters (Meyer et al. 2000; Sondergeld et al. 2005). The transition temperature is 125 K in natural samples but becomes 155 K in a deuterated sample, showing that the predominant mechanism must be proton (or deuterium) ordering (Carpenter et al. 2003). There is thus no evidence for a separation of displacive and order/disorder contributions in this case.

### Interpretation of the phase transitions in lawsonite

From comparisons of the new RUS data presented here with previous studies on lawsonite, it is proposed that there are three important dissipation processes associated with the two phase transitions in lawsonite.

Dissipation immediately below the 125 K transition appears to be directly associated with a classical ferroelectric transition driven by the static displacement of protons. Dynamical effects responsible for the dissipation could then simply be due to atomic motions between symmetry-related crystallographic sites when the energy barrier between them is low.

The anomalies in strain, elasticity, dissipation, and IR absorption seen in the temperature range ~210–220 K are unusual as they are not at a phase transition and lie well within the stability range of the *Pmcn* structure. It is suggested here that these anomalies are due to structural changes in the sample that are related to the 270 K phase transition but are not responsible for it. A likely mechanism is a change in the dynamical motions of protons either in the $H_2O$ groups or in the OH groups between their split sites in the *Pmcn* structure.

Anomalies in properties at ~250 K are similar to those found at ~210–220 K but are more prominent. It is most likely that the behavior at ~250 K is related to the major proton order-disorder process associated with the 270 K transition. Both dissipation processes, at ~220 and at ~250 K, are separated from the transition temperature, consistent with the view that proton ordering and framework displacements contribute separately to the phase transition itself. The implication is that two different species of protons (OH and $H_2O$) order on different timescales at different temperatures, and therefore give rise to two separate peaks in the dissipation.

## Acknowledgments

Ruth E.A. McKnight was supported by a studentship from the Engineering and Physical Sciences Research Council (grant no. EPSRC DTG05 10026782). The RUS equipment was built with a grant from the National Environmental Research Council of Great Britain (grant no. NER/A/S/2000/01055), which is gratefully acknowledged.

## References cited

Cámara, F., Doukhan, J.C., and Carpenter, M.A. (2001) Lattice defects in lawsonite: A TEM investigation. Mineralogical Magazine, 65, 33–39.

Carpenter, M.A. (2006) Elastic properties of minerals and the influence of phase transitions. American Mineralogist, 91, 229–246.

Carpenter, M.A., Meyer, H.-M., Sondergeld, P., Marion, S., and Knight, K.S. (2003) Spontaneous strain variations through the low temperature phase transitions of deuterated lawsonite. American Mineralogist, 88, 534–546.

Chatterjee, N.C. and Leistner, H. (1984) The system $CaO-Al_2O_3-SiO_2-H_2O$. New phase equilibria data, some calculated phase relations and their petrological significance. Contributions to Mineralogy and Petrology, 88, 1–13.

Hayward, S.A., Burriel, R., Marion, S., Meyer, H.-M., and Carpenter, M.A. (2002) Kinetic effects associated with the low-temperature phase transitions in lawsonite. European Journal of Mineralogy, 14, 1145–1153.

Leisure, R.G. and Willis, F.A. (1997) Resonant ultrasound spectroscopy. Journal of Physics: Condensed Matter, 9, 6001–6029.

Leisure, R.G., Foster, K., Hightower, J.E., and Agosta, D.S. (2004) Internal friction studies by resonant ultrasound spectroscopy. Materials Science and Engineering, A370, 34–40.

Libowitzky, E. and Armbruster, T. (1995) Low-temperature phase transitions and the role of hydrogen bonds in lawsonite. American Mineralogist, 80, 1277–1285.

Libowitzky, E. and Rossman, G.R. (1996) FTIR spectroscopy of lawsonite between 82 and 325 K. American Mineralogist, 81, 1080–1091.

Martín-Olalla, J.-M., Hayward, S.A., Meyer, H.-M., Ramos, S., del Cerro, J., and Carpenter, M.A. (2001) Phase transitions in lawsonite: a calorimetric study. European Journal of Mineralogy, 13, 5–14.

Maynard, J.D. (1996) Resonant ultrasound spectroscopy. Physics Today, 49, 26–31.

Meyer, H.-M., Carpenter, M.A., Graeme-Barber, A., Sondergeld, P., and Schranz, W. (2000) Local and macroscopic order parameter variations associated with low temperature phase transitions in lawsonite, $CaAl_2Si_2O_7(OH)_2{\cdot}H_2O$. European Journal of Mineralogy, 12, 1139–1150.

Meyer, H.-M., Marion, S., Sondergeld, P., Carpenter, M.A., Knight, K.S., Redfern, S.A.T., and Dove, M.T. (2001) Displacive components of the low-temperature phase transitions in lawsonite. American Mineralogist, 86, 566–577.

Migliori, A. and Maynard, J.D. (2005) Implementation of a modern resonant ultrasound spectroscopy system for the measurement of the elastic moduli of small solid specimens. Review of Scientific Instruments, 76, 121301.

Migliori, A. and Sarrao, J.L. (1997) Resonant Ultrasound Spectroscopy: Applications to Physics, Material Measurements and Nondestructive Evaluation, 201 p. John Wiley and Sons Inc., New York.

Migliori, A., Sarrao, J.L., Visscher, W.M., Bell, T.M., Lei, M., Fisk, Z., and Leisure, R.G. (1993) Resonant ultrasound spectroscopic techniques for measurement of the elastic moduli of solids. Physica B, 183, 1–24.

Migliori, A., Darling, T.W., Baiardo, J.P., and Freibert, F. (2001) Resonant Ultrasound Spectroscopy (RUS). In M. Levy, H. Bass, and R. Stern, Eds., Handbook of Elastic Properties of Solids, Liquids, and Gases, I, p. 239–262. Academic Press, New York.

Nowick, A.S. and Berry, B.S., Eds. (1972) Anelastic Relaxation in Crystalline Solids, p. 226–246 (The Snoek Relaxation). Academic Press, New York.

Pawley, A.R. (1994) The pressure and temperature stability limits of lawsonite: Implications for $H_2O$ recycling in subduction zones. Contributions to Mineralogy and Petrology, 118, 99–108.

Pawley, A.R., Redfern, S.A.T., and Holland, T.J.B. (1996) Volume behavior of hydrous minerals at high pressure and temperature: I. Thermal expansion of lawsonite, zoisite, clinzoisite, and diaspore. American Mineralogist, 81, 335–340.

Schilling, F.R., Sinogeikin, S.V., and Bass, J.D. (2003) Single-crystal elastic properties of lawsonite and their variation with temperature. Physics of the Earth and Planetary Interiors, 136, 107–118.

Schmidt, M.W. (1995) Lawsonite: upper pressure stability and formation of higher density hydrous phases. American Mineralogist, 80, 1286–1292.

Schmidt, M.W. and Poli, S. (1998) Experimentally base water budgets for dehydrating slabs and consequences for arc magma generation. Earth and Planetary Science Letters, 163, 361–379.

Schranz, W., Tröster, A., Gardon, M., Krexner, G., Prem, M., Carpenter, M.A., Sondergeld, P., and Armbruster, T. (2005) Crossover from classical to 3d-Ising critical behaviour near the antiferrodistortive phase transition of lawsonite. Zeitschrift fur Kristallographie, 220(8), 704–711.

Schreuer, J. (2006) Elastic properties of mullite single crystals up to 1400 °C. Journal of the American Ceramic Society, 89(5), 1624–1631.

Schreuer, J. and Thybaut, C. (2005) Anelastic relaxation effects and elastic instabilities in CGG-type compounds. Proceedings of the IEEE Ultrasonics Symposium 2005, 695–698.

Schreuer, J., Thybaut, T., Prestat, M., Stade, J., and Haussühl, E. (2003) Towards an understanding of the anomalous electromechanical behavior of langasite and related compounds at high temperatures. Proceedings of the IEEE Ultrasonics Symposium 2003, 196–199.

Sinogeikin, S.V., Schilling, F.R., and Bass, J.D. (2000) Single crystal elasticity of lawsonite. American Mineralogist, 85, 1834–1837.

Snoek, J.L. (1941) Effect of small quantities of carbon and nitrogen on the elastic and plastic properties of iron. Physica VIII, 7, 711–733.

Sondergeld, P., Schranz, W., Kityk, A.V., Carpenter, M.A., and Libowitzky, E. (2000a) Ordering behaviour of the mineral lawsonite. Phase Transitions, 71, 189–203.

Sondergeld, P., Schranz, W., Tröster, A., Carpenter, M.A., Libowitzky, E., and Kityk, A.V. (2000b) Optical, elastic, and dielectric studies of phase transitions in lawsonite. Physical Review B, 62, 6143–6147.

Sondergeld, P., Schranz, W., Tröster, A., Armbruster, T., Giester, G., Kityk, A., and Carpenter, M.A. (2005) Ordering and elasticity associated with low-temperature phase transitions in lawsonite. American Mineralogist, 90, 448–456.

Manuscript received January 18, 2007
Manuscript accepted June 18, 2007
Manuscript handled by Guoyin Shen